

Gas Column Density

5 Mpc

Stellar Column Density

5 Mpc



# Elusive diffuse $\gamma$ -ray emission in galaxy clusters: the role of CR transport

*Paper submitted to Nature Astronomy: Efficient micromirror confinement of sub-TeV cosmic rays in galaxy clusters*  
<https://arxiv.org/abs/2311.01497>

Patrick Reichherzer<sup>1</sup>, 2023/11

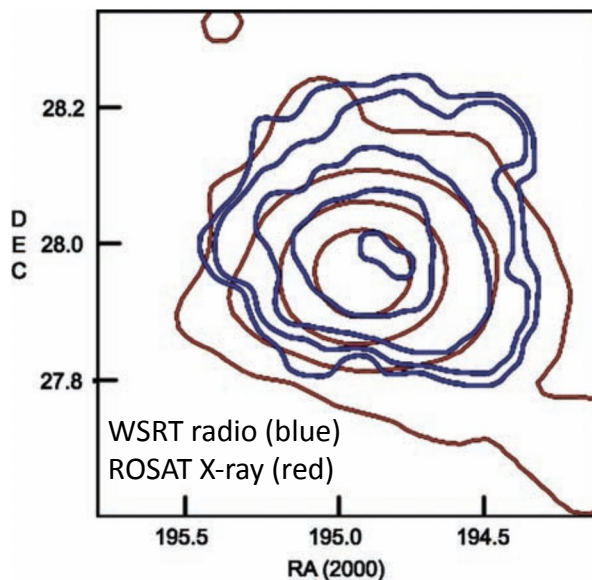
with:

A. Bott<sup>1</sup>, R. Ewart<sup>1</sup>, G. Gregori<sup>1</sup>, P. Kempster<sup>2</sup>, M. Kunz<sup>2</sup>, and A. Schekochihin<sup>1</sup>

<sup>1</sup> University of Oxford    <sup>2</sup> Princeton University

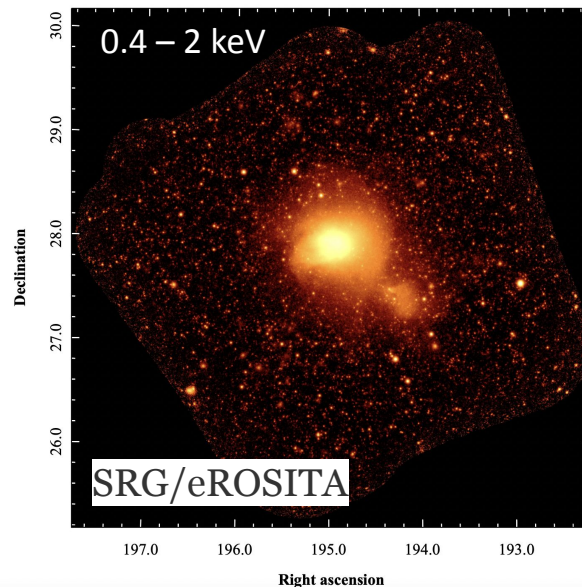
# Non-ambiguous detection of diffuse $\gamma$ -ray emission still elusive

Radio & X-rays



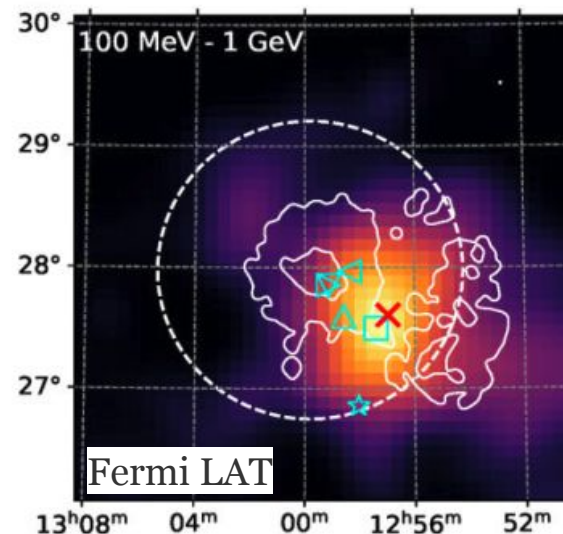
Brown & Rudnick (2014)

X-rays

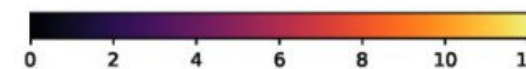
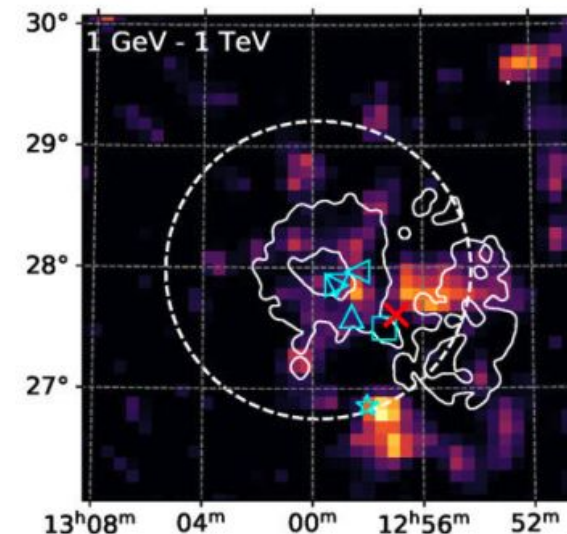


Churazov et al. (2021)

$\gamma$ -rays



RA (J2000)



Baghmanyant et al. (2022)

← diffuse emission

non-ambiguous detection of diffuse  $\gamma$ -ray emission elusive →

- ❑ Differences in morphology due to
  - ❑ emitting particle types (thermal plasma vs. CRs)
  - ❑ source distributions of emitting particles
  - ❑ **transport of emitting particles (streaming, diffusing, (quasi-)ballistic)**

# Scale hierarchy in galaxy clusters relevant for CR transport

The most massive galaxy cluster merger in the **TNG-Cluster simulation** at redshift 0. The total halo mass is  $1e15.2$  solar masses

<https://www.tng-project.org/dev707/cluster/>

*A. Pillepich et al. (2023)*

*D. Nelson et al. (2023)*

*W. Lee et al. (2023)*

...

Gas Column Density

5 Mpc

A simulation snapshot showing the gas column density in a galaxy cluster merger. The color scale ranges from dark purple (low density) to bright green and yellow (high density). The central region shows a complex, multi-lobed structure with high density, indicating the merger of two clusters. The density decreases towards the edges. A white scale bar in the bottom right corner indicates 5 Mpc.

Stellar Column Density

5 Mpc

A simulation snapshot showing the stellar column density in the same galaxy cluster merger. The stars are represented as small orange and yellow dots. The distribution of stars follows the same complex, multi-lobed structure as the gas, with a high concentration in the central region. A white scale bar in the bottom right corner indicates 5 Mpc.

# Scale hierarchy in galaxy clusters relevant for CR transport

The most massive galaxy cluster merger in the TNG-Cluster simulation at redshift 0. The total halo mass is  $1e15.2$  solar masses

<https://www.tng-project.org/dev707/cluster/>

A. Pillepich et al. (2023)

D. Nelson et al. (2023)

W. Lee et al. (2023)

...

Gas Column Density

5 Mpc

Stellar Column Density

5 Mpc

Temperature

$T = \text{few keV}$

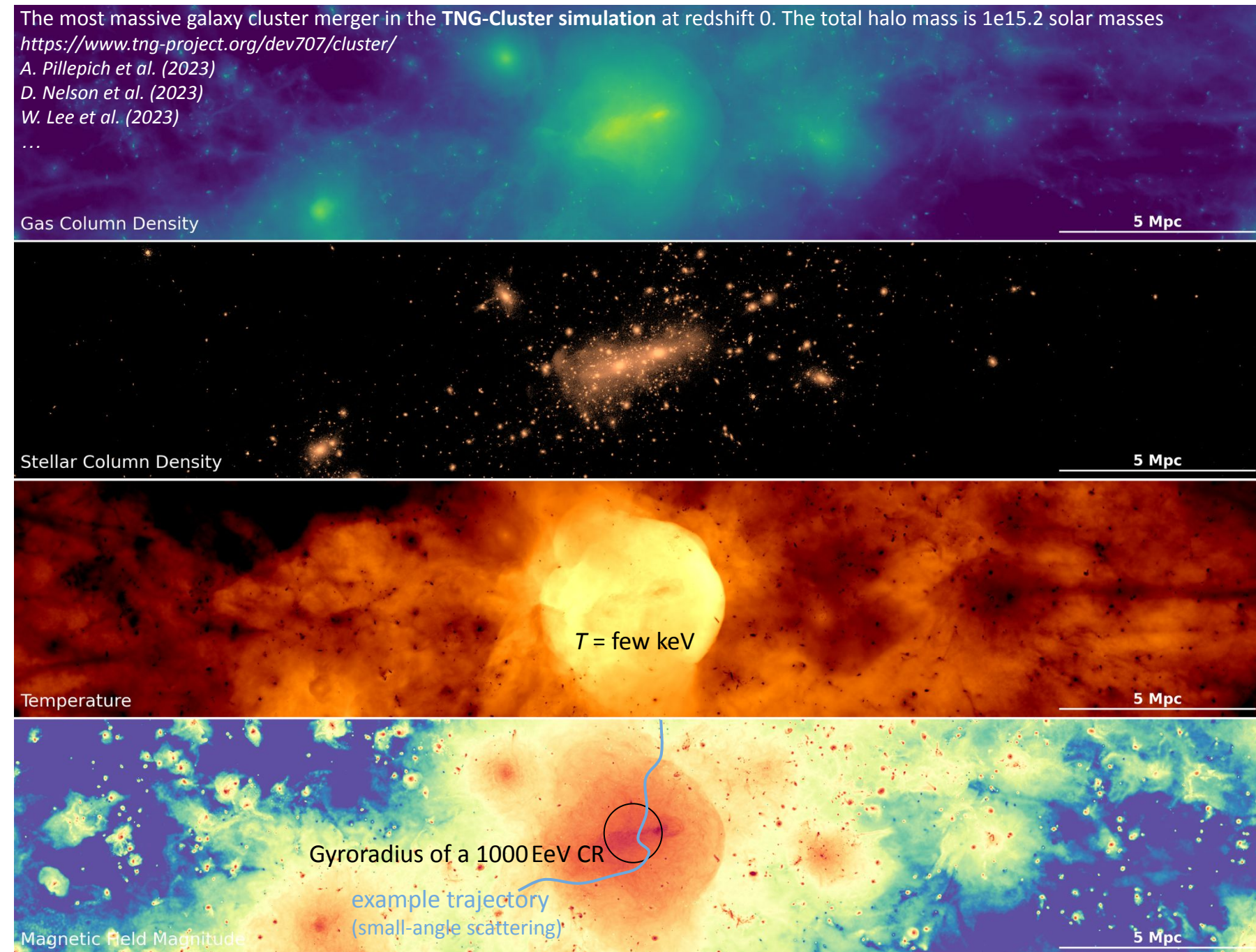
5 Mpc

Magnetic Field Magnitude

Gyroradius of a 1000 EeV CR

example trajectory  
(small-angle scattering)

5 Mpc



# Scale hierarchy in galaxy clusters relevant for CR transport

The most massive galaxy cluster merger in the TNG-Cluster simulation at redshift 0. The total halo mass is  $1e15.2$  solar masses

<https://www.tng-project.org/dev707/cluster/>

A. Pillepich et al. (2023)

D. Nelson et al. (2023)

W. Lee et al. (2023)

...

Gas Column Density

5 Mpc

Stellar Column Density

5 Mpc

Temperature

$T = \text{few keV}$

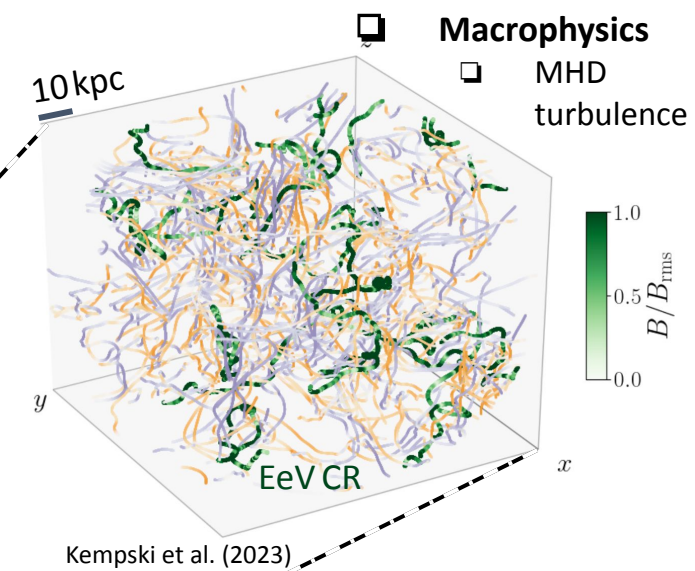
5 Mpc

Magnetic Field Magnitude

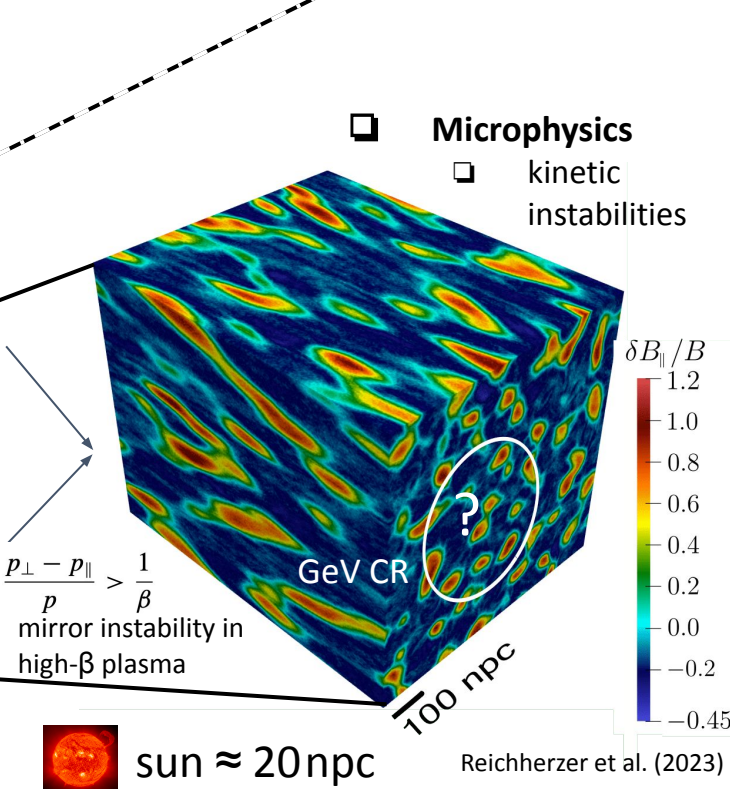
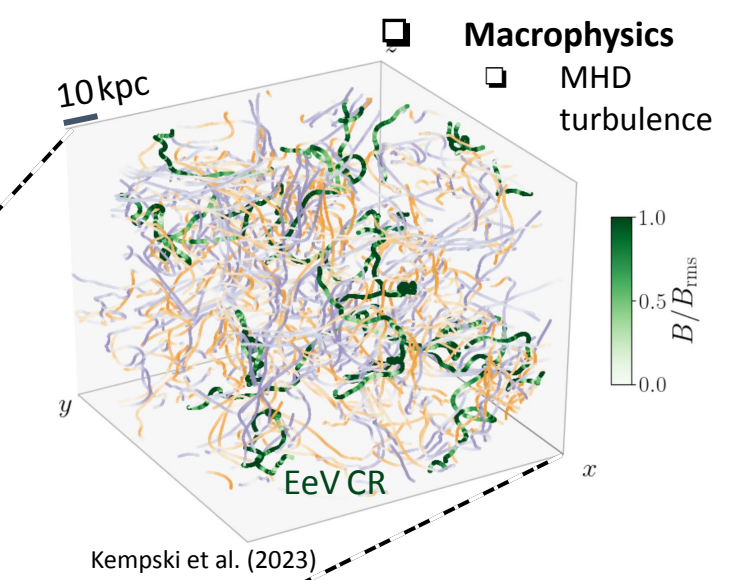
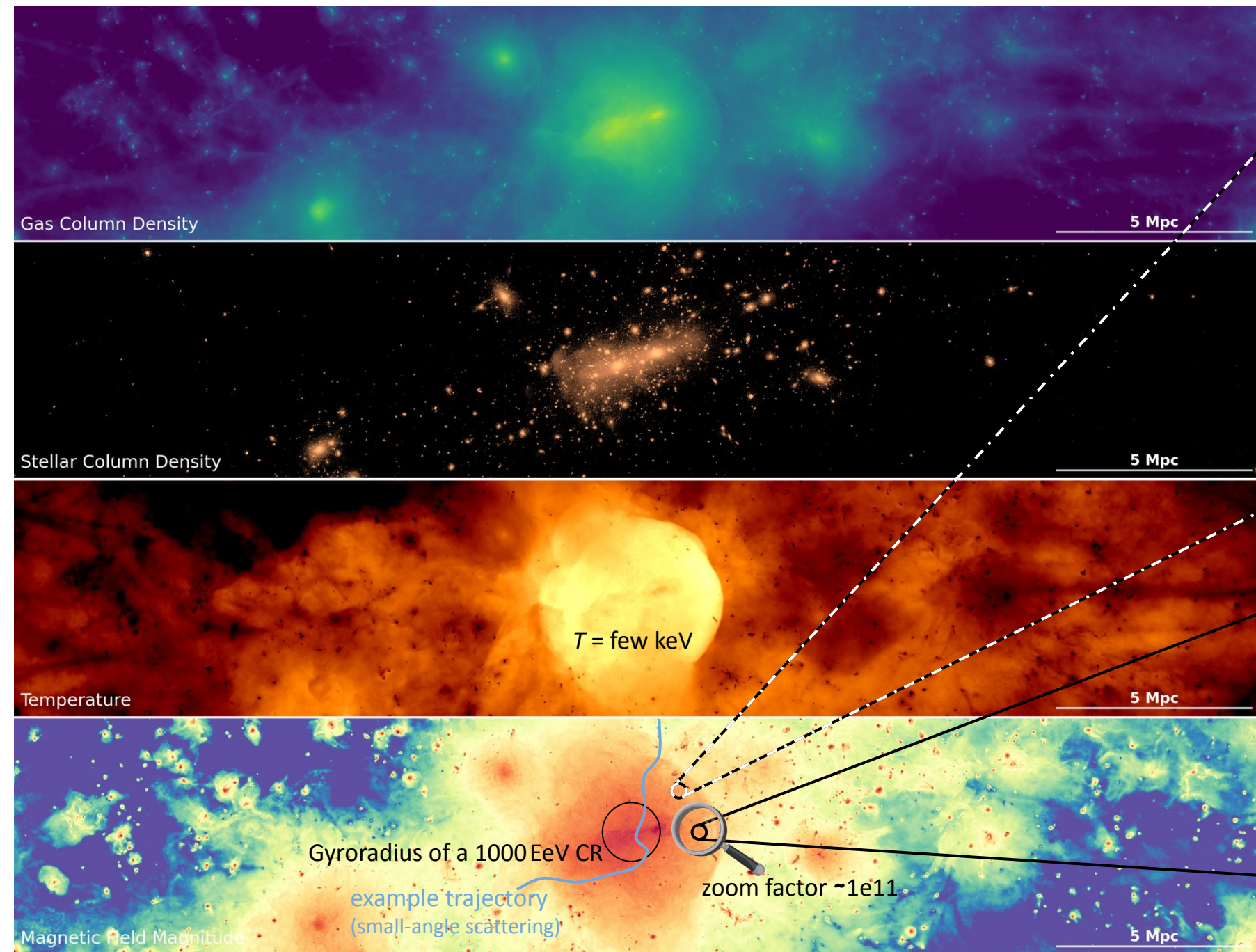
Gyroradius of a 1000 EeV CR

example trajectory  
(small-angle scattering)

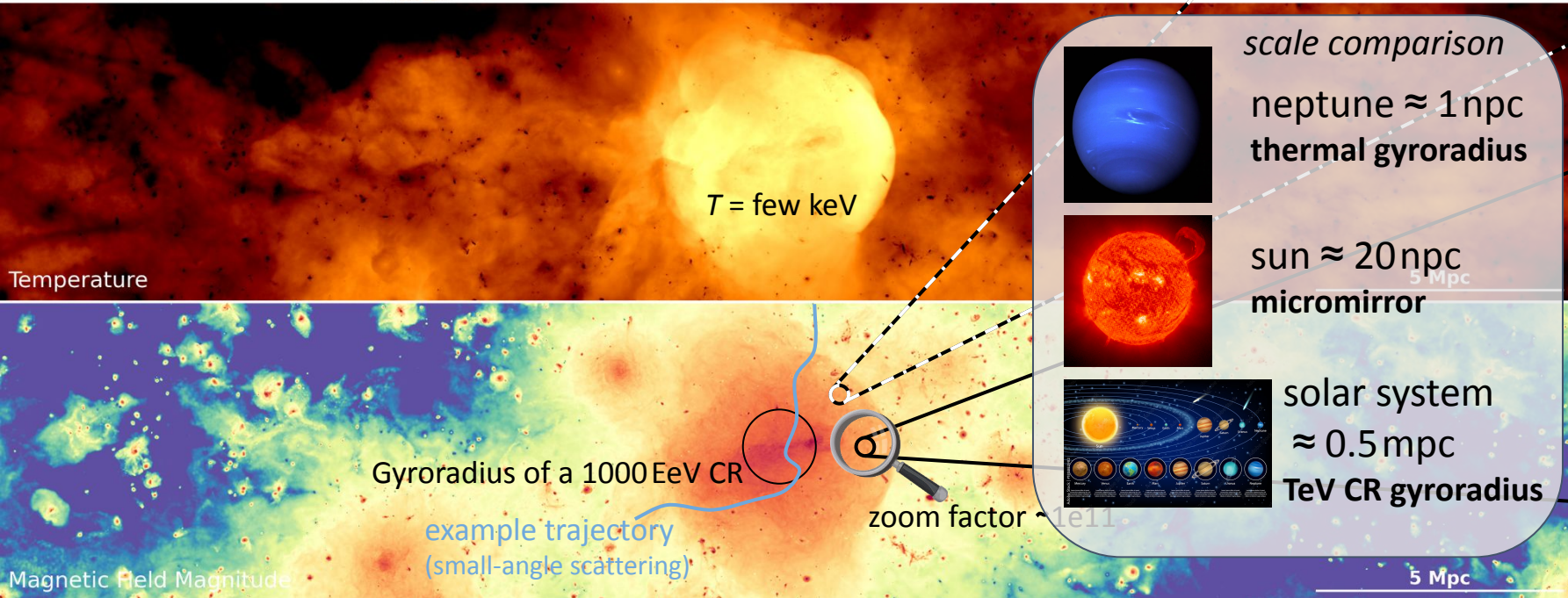
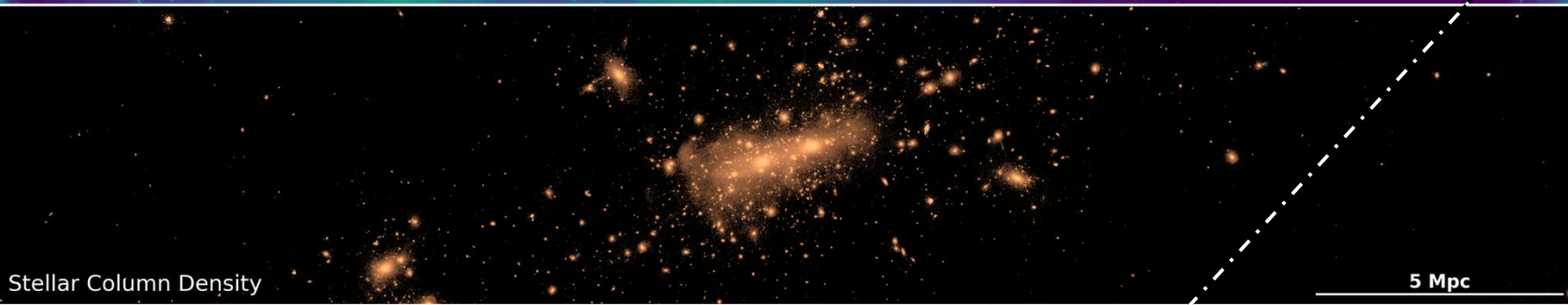
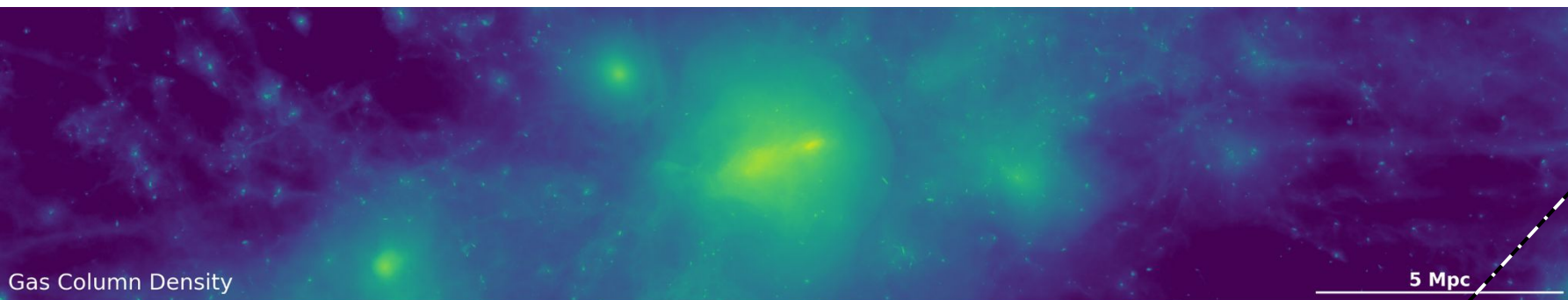
5 Mpc



# Scale hierarchy in galaxy clusters relevant for CR transport

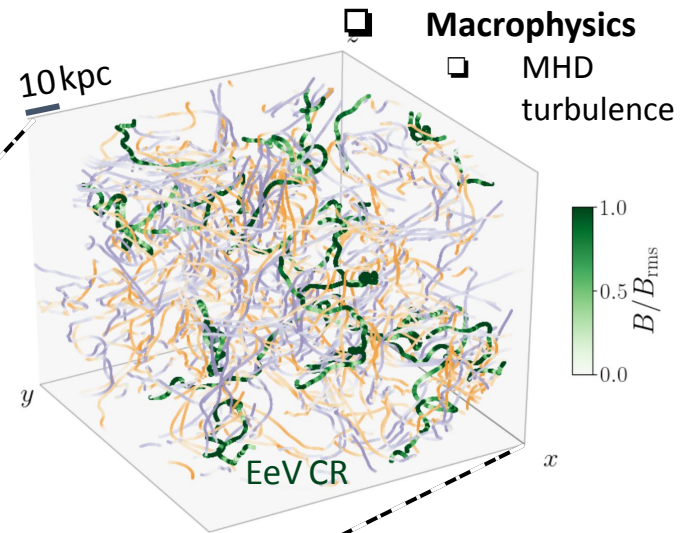


# Scale hierarchy in galaxy clusters relevant for CR transport

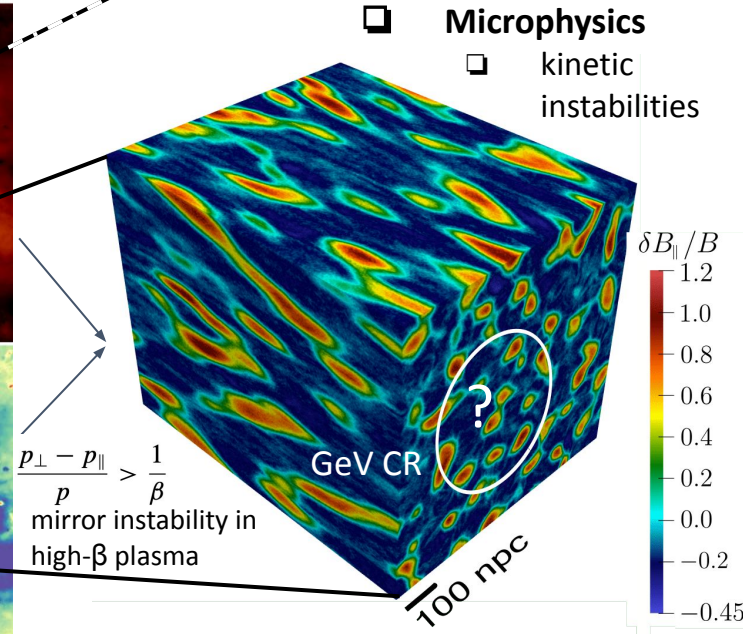


*scale comparison*

- neptune  $\approx 1 \text{ npc}$
- thermal gyroradius
- sun  $\approx 20 \text{ npc}$
- micromirror
- solar system  $\approx 0.5 \text{ mpc}$
- TeV CR gyroradius

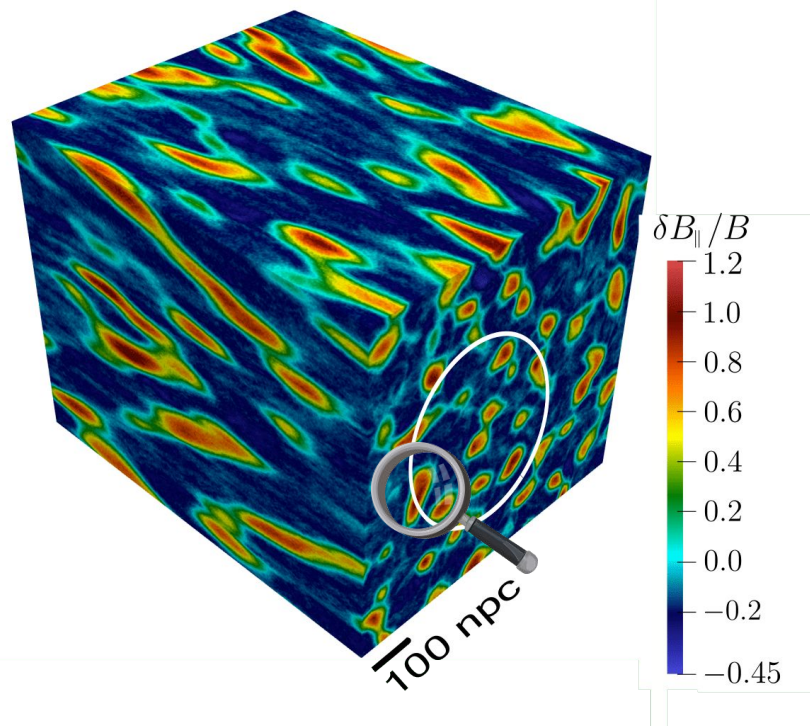


Kempski et al. (2023)

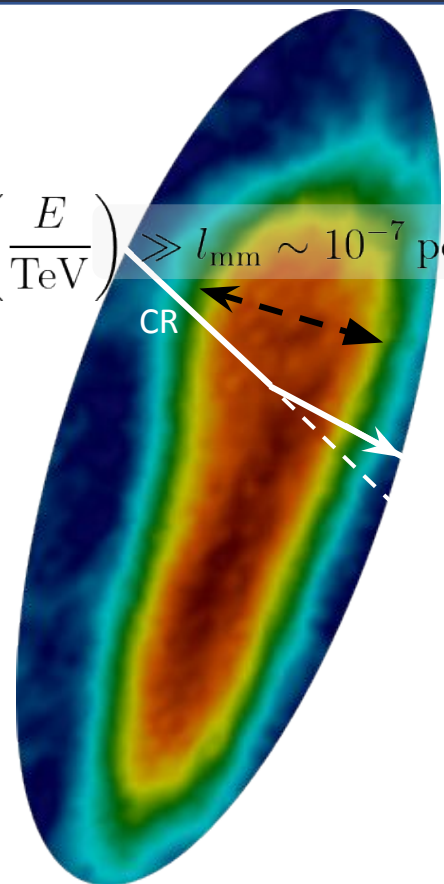


Reichherzer et al. (2023)

# Effect of micromirrors on large-scale CR transport



$$r_g \sim 10^{-4} \text{ pc} \left( \frac{E}{\text{TeV}} \right) \gg l_{\text{mm}} \sim 10^{-7} \text{ pc}$$



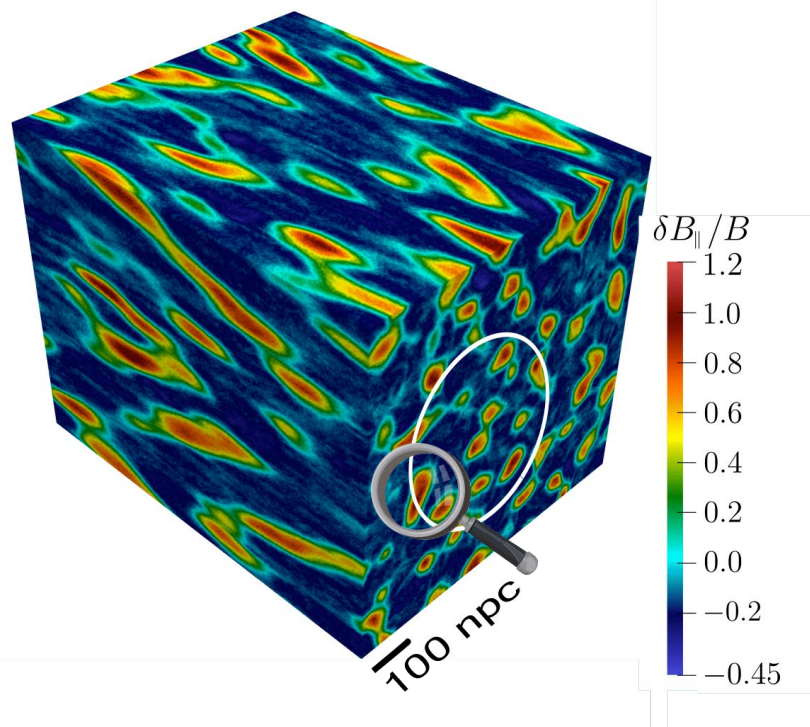
Deflection in micromirror:

$$\delta \mathbf{v} \sim \frac{q}{\gamma m c v} \int_0^{l_{\text{mm}}} dl \mathbf{v} \times \delta \mathbf{B}_{\text{mm}}$$

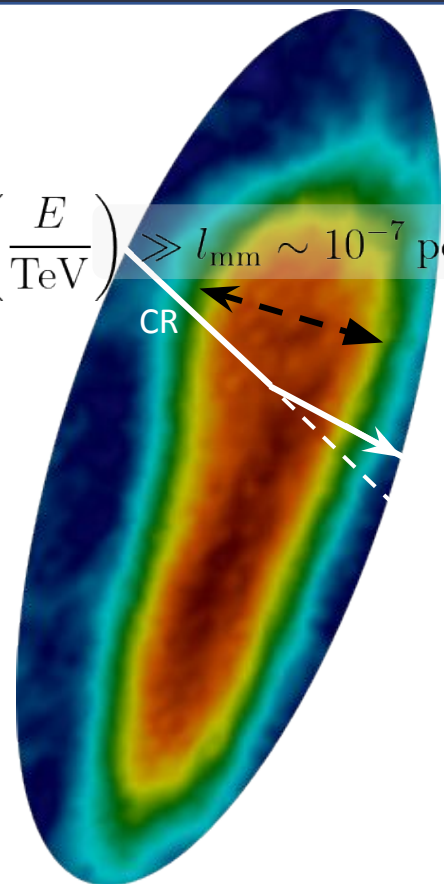
$$\delta \Theta \sim \frac{|\delta \mathbf{v}|}{c} \sim \frac{l_{\text{mm}}}{r_g} \frac{\delta B_{\text{mm}}}{B}$$



# Effect of micromirrors on large-scale CR transport



$$r_g \sim 10^{-4} \text{ pc} \left( \frac{E}{\text{TeV}} \right) \gg l_{\text{mm}} \sim 10^{-7} \text{ pc}$$



Deflection in micromirror:

$$\delta \mathbf{v} \sim \frac{q}{\gamma m c v} \int_0^{l_{\text{mm}}} dl \mathbf{v} \times \delta \mathbf{B}_{\text{mm}}$$

$$\delta \Theta \sim \frac{|\delta \mathbf{v}|}{c} \sim \frac{l_{\text{mm}}}{r_g} \frac{\delta B_{\text{mm}}}{B}$$

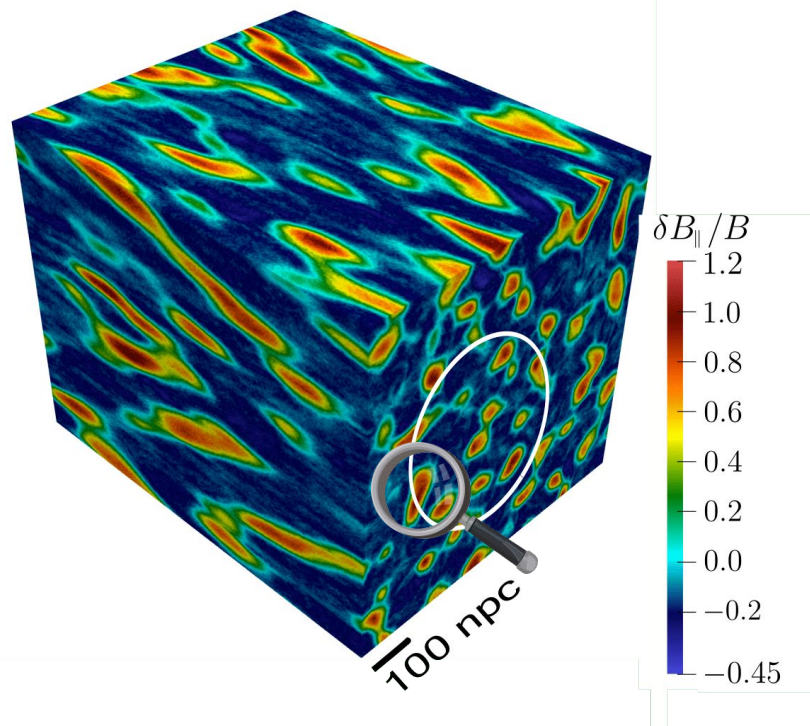
Assuming that these deflections add up as random walk, the scattering rate is

$$\nu_{\text{mm}} \sim \frac{\delta \Theta^2}{\delta t} \sim \frac{c l_{\text{mm}}}{r_g^2} \left( \frac{\delta B_{\text{mm}}}{B} \right)^2,$$

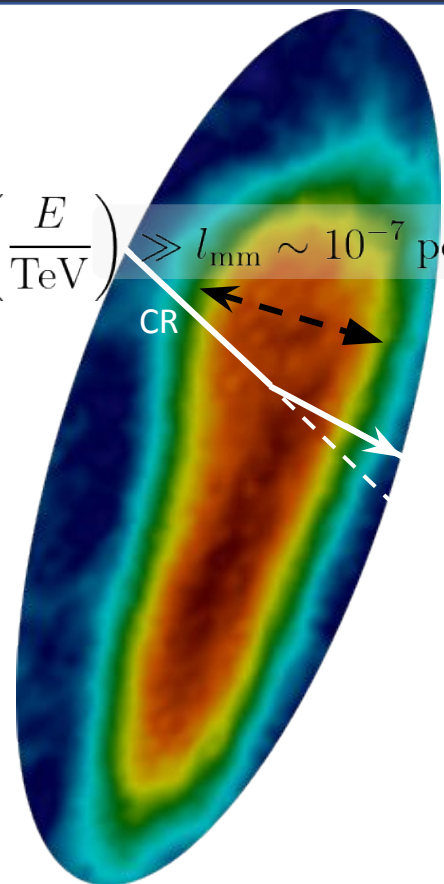
which implies a spatial diffusion coefficient of

$$\kappa_{\text{mm}} \sim \frac{c^2}{\nu_{\text{mm}}} \sim \frac{c r_g^2}{l_{\text{mm}}} \left( \frac{\delta B_{\text{mm}}}{B} \right)^{-2} \propto E^2 l_{\text{mm}}^{-1}.$$

# Effect of micromirrors on large-scale CR transport



$$r_g \sim 10^{-4} \text{ pc} \left( \frac{E}{\text{TeV}} \right) \gg l_{\text{mm}} \sim 10^{-7} \text{ pc}$$



Deflection in micromirror:

$$\delta \mathbf{v} \sim \frac{q}{\gamma m c v} \int_0^{l_{\text{mm}}} dl \mathbf{v} \times \delta \mathbf{B}_{\text{mm}}$$

$$\delta \Theta \sim \frac{|\delta \mathbf{v}|}{c} \sim \frac{l_{\text{mm}}}{r_g} \frac{\delta B_{\text{mm}}}{B}$$

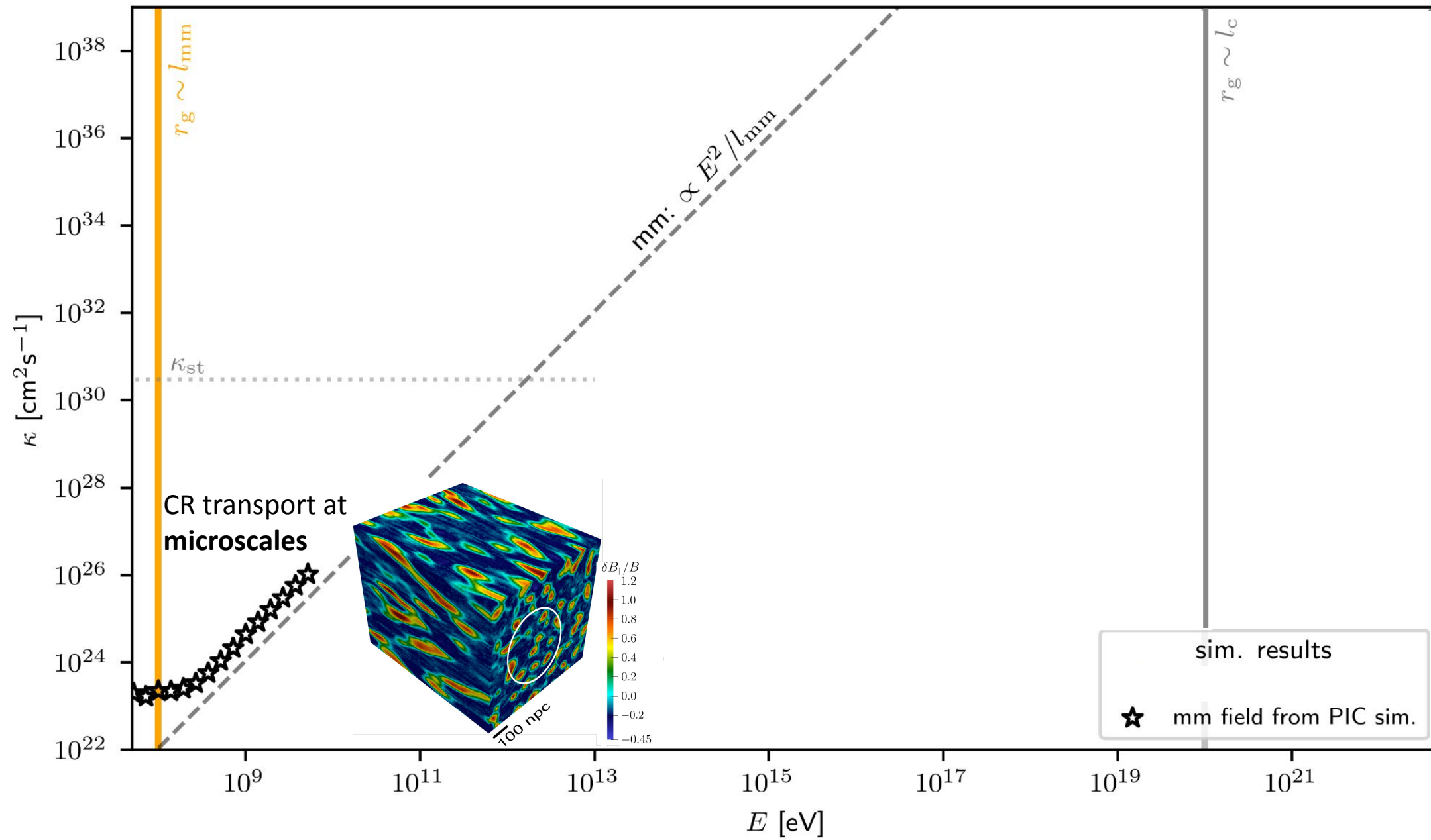
Assuming that these deflections add up as random walk, the scattering rate is

$$\nu_{\text{mm}} \sim \frac{\delta \Theta^2}{\delta t} \sim \frac{c l_{\text{mm}}}{r_g^2} \left( \frac{\delta B_{\text{mm}}}{B} \right)^2,$$

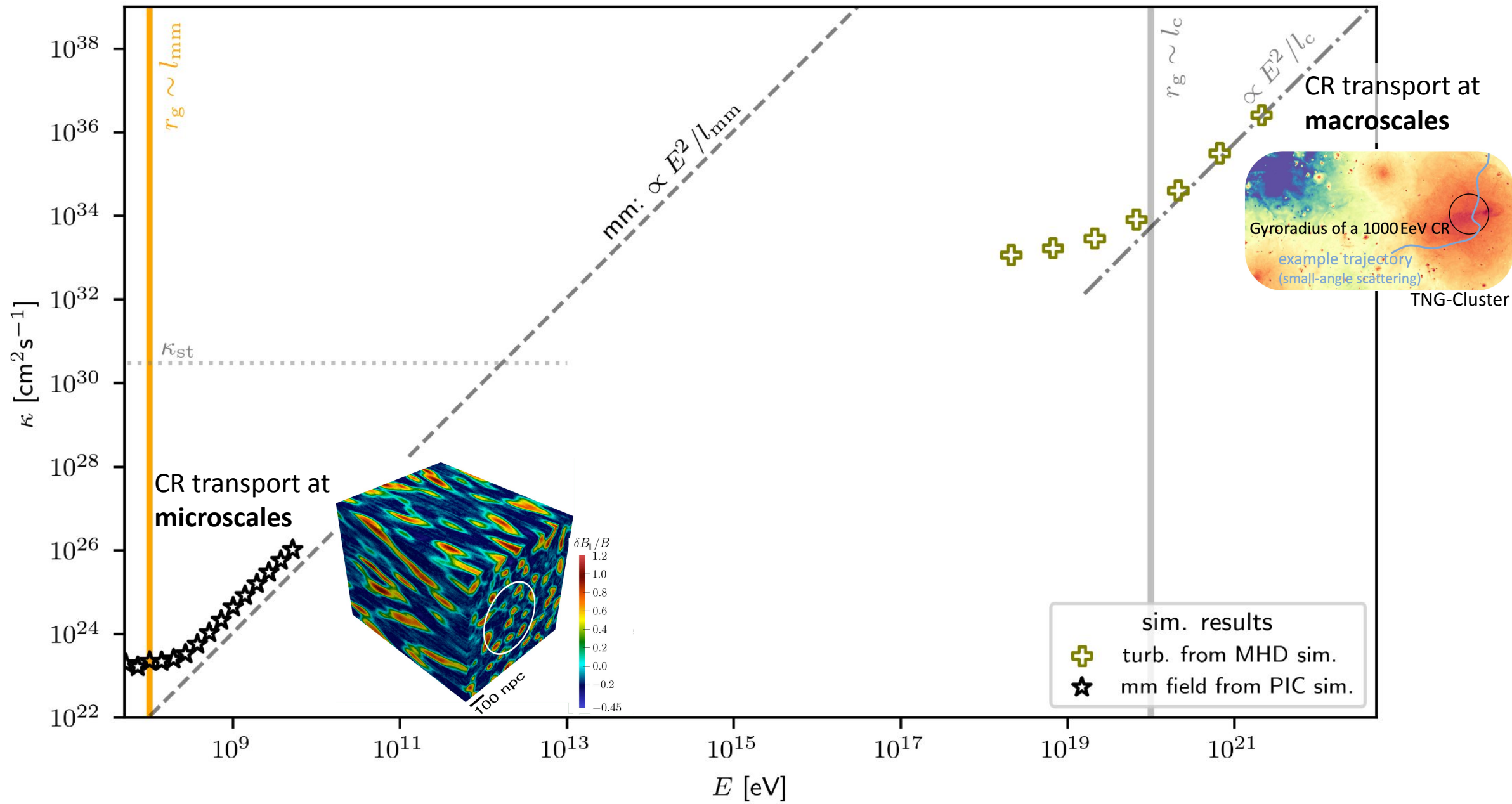
which implies a spatial diffusion coefficient of

$$\kappa_{\text{mm}} \sim 10^{30} Z^{-2} \left( \frac{T}{5 \text{ keV}} \right)^{-1/2} \left( \frac{B}{3 \mu\text{G}} \right)^{-1} \left( \frac{\delta B_{\text{mm}}/B}{1/3} \right)^{-2} \left( \frac{E}{\text{TeV}} \right)^2 \text{ cm}^2 \text{ s}^{-1}$$

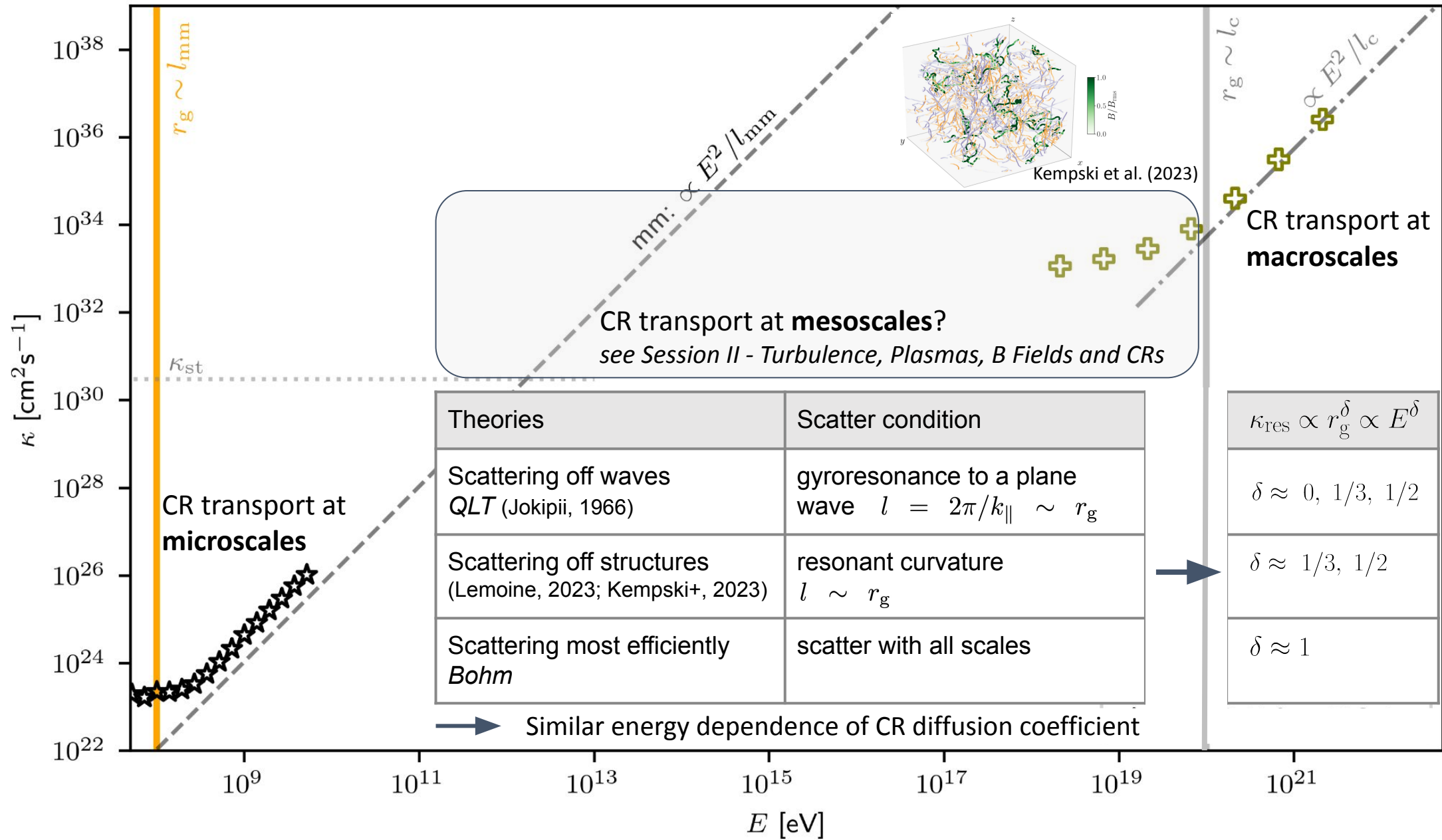
# CR transport regimes in ICM



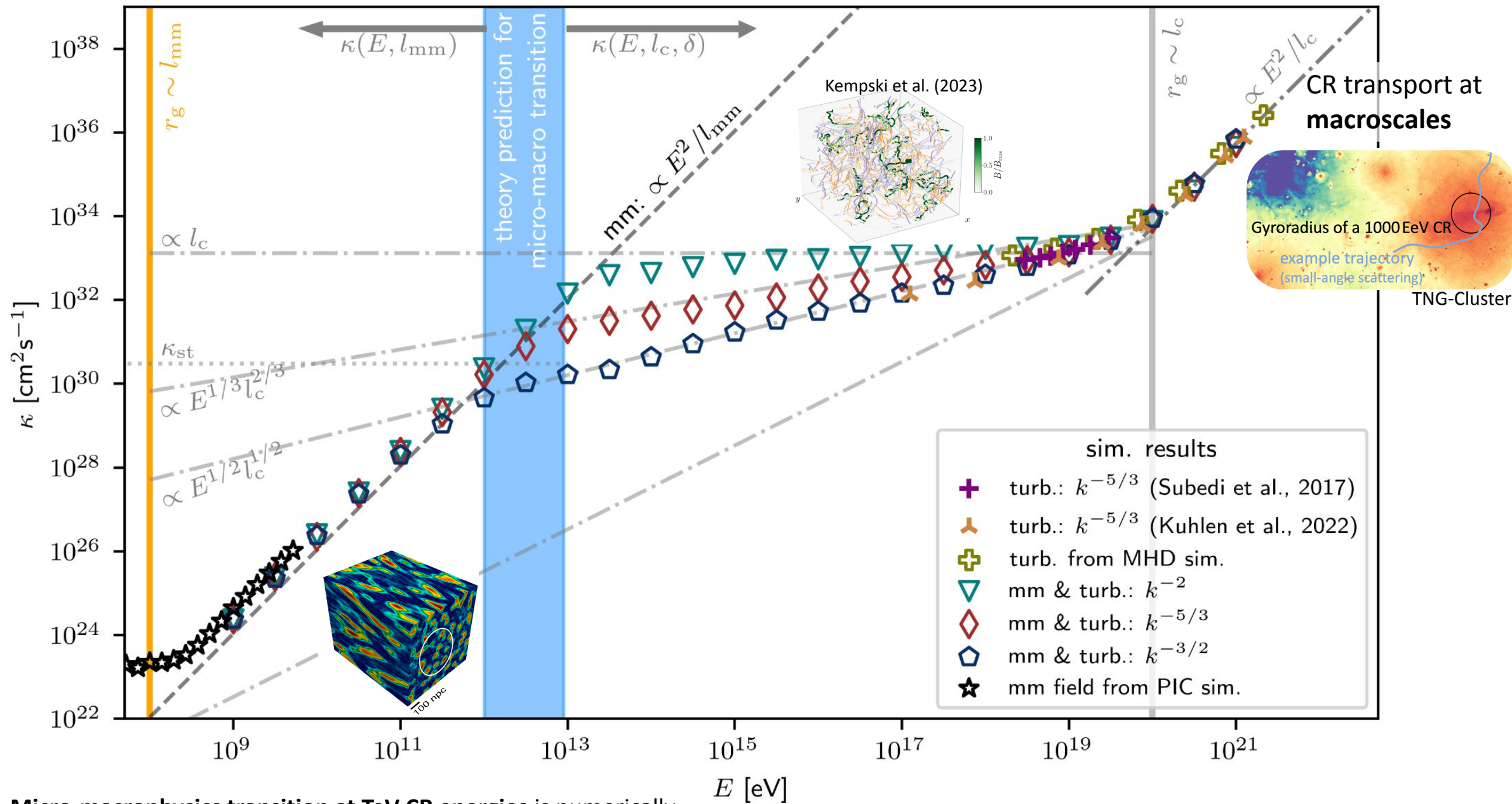
# CR transport regimes in ICM



# CR transport regimes in ICM



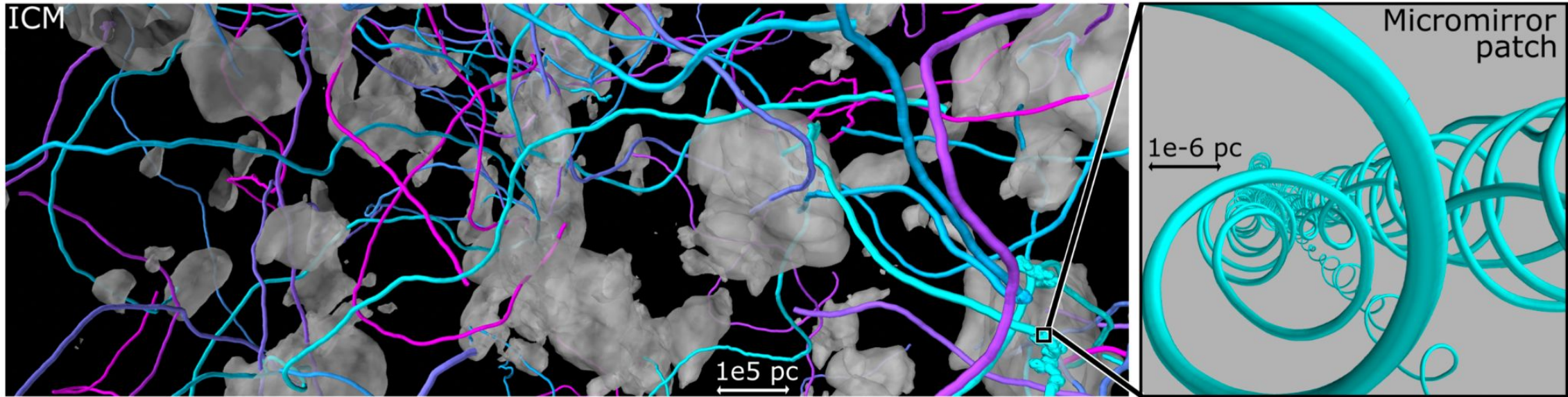
# CR transport regimes in ICM



➔ **Micro-macrophysics transition at TeV CR energies** is numerically confirmed using synthetic turbulence. We use PIC and MHD to validate the consistency of our numerical approach at micro and macroscales.

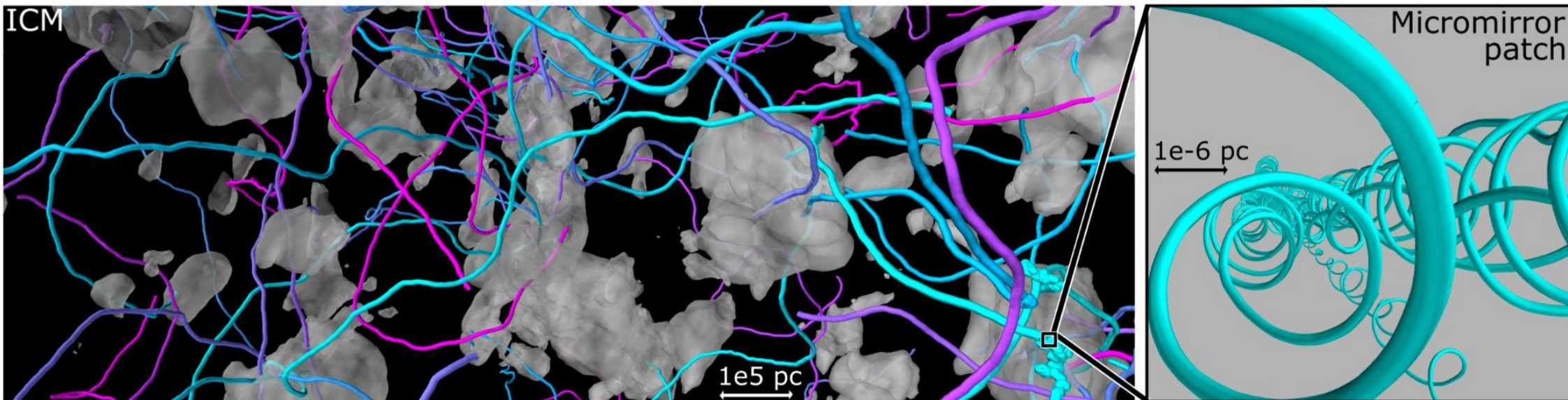
## Case of spatially intermittent micromirrors

In reality: micromirrors form only where turbulence causes local magnetic field amplification strong enough to generate a pressure anisotropy beyond the mirror-instability threshold → we turn micromirror scattering on only if the CR is seeing a magnetic field above a certain threshold



## Case of spatially intermittent micromirrors

In reality: micromirrors form only where turbulence causes local magnetic field amplification strong enough to generate a pressure anisotropy beyond the mirror-instability threshold  $\rightarrow$  we turn micromirror scattering on only if the CR is seeing a magnetic field above a certain threshold



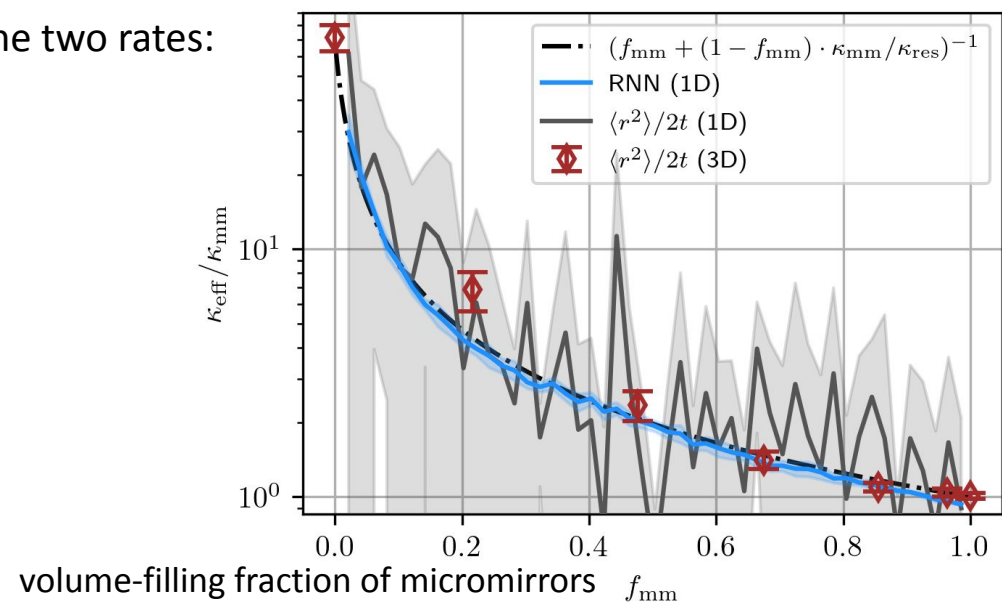
The effective scattering rate in a two-phase medium is the average of the two rates:

$$\nu_{\text{eff}} \sim f_{\text{mm}} \nu_{\text{mm}} + (1 - f_{\text{mm}}) \nu_{\text{res}}$$

Then the effective diffusion coefficient is:

$$\kappa_{\text{eff}} \sim \frac{\kappa_{\text{mm}}}{f_{\text{mm}} + (1 - f_{\text{mm}}) \kappa_{\text{mm}} / \kappa_{\text{res}}}$$

$\rightarrow$  Only minor modification of our cruder ( $f_{\text{mm}} = 1$ ) estimate





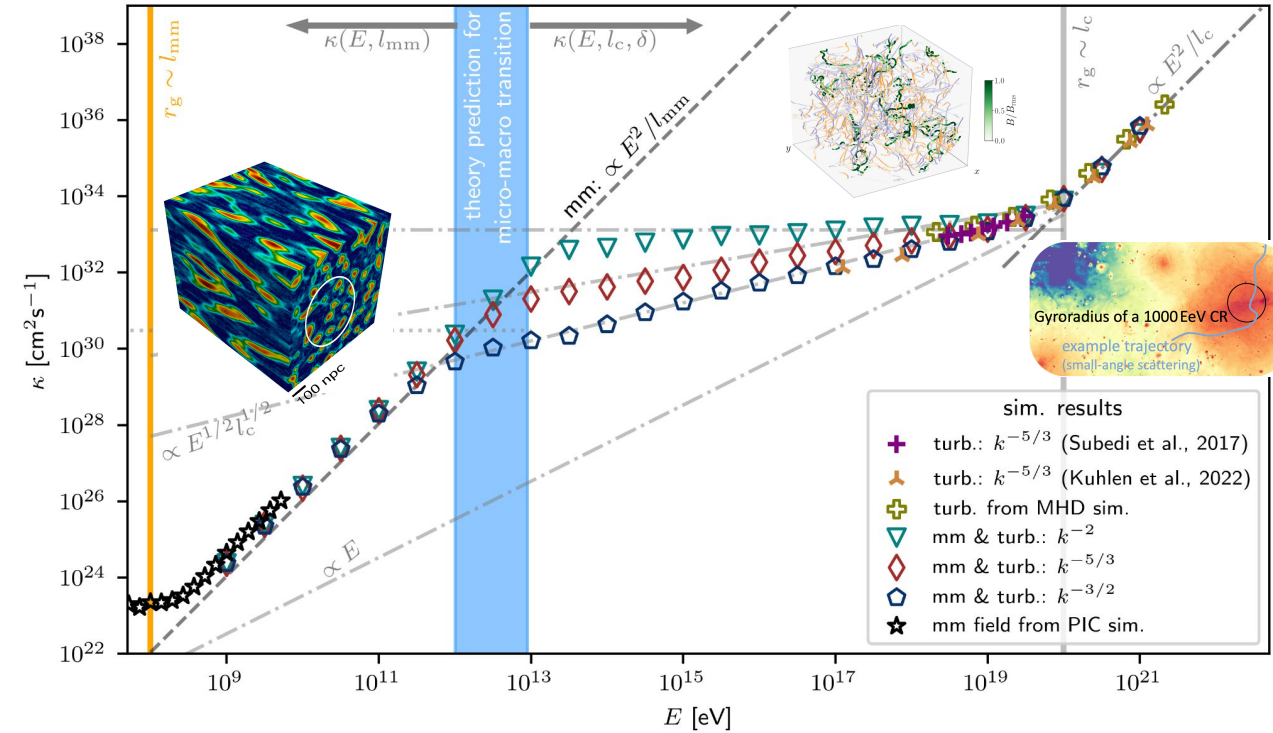
## Results:

- Effect on macroscopic sub-TeV CR diffusion from magnetic micromirrors

$$\kappa_{\text{mm}} \sim 10^{30} \text{cm}^2 \text{s}^{-1} \left( \frac{l_{\text{mm}}}{100 \text{npc}} \right)^{-1} \left( \frac{B}{3 \mu\text{G}} \right)^{-2} \left( \frac{\delta B_{\text{mm}}/B}{1/3} \right)^{-2} \left( \frac{E}{\text{TeV}} \right)^2$$

- Minor modification of only considering patches of micromirrors

$$\kappa_{\text{eff}} \sim \frac{\kappa_{\text{mm}}}{f_{\text{mm}} + (1 - f_{\text{mm}})\kappa_{\text{mm}}/\kappa_{\text{res}}}$$



Implications of increased collisionality (suppressed diffusion coefficients) in high- $\beta$  plasmas:

- Traps sub-TeV CRs near emission sources within galaxy clusters, addressing non-detection of diffuse  $\gamma$ -ray emission**

$$\frac{\gamma_{\text{SI}}}{\nu_{\text{mm}}} \sim 4 \times 10^{-5} \left( \frac{B}{3 \mu\text{G}} \right)^{-1} \left( \frac{E}{\text{TeV}} \right)^{0.4} \left( \frac{l_{\text{mm}}}{100 \text{npc}} \right)^{-1} \left( \frac{\delta B_{\text{mm}}/B}{1/3} \right)^{-2}$$

- Potential suppression of the CR streaming instability
- CRs being “frozen” within the plasma as gas density and magnetic field evolve
  - a presumption already used in models of dynamic evolution of galaxy clusters



paper link



1. The growth rate of the resonant streaming instability is:

$$\gamma_{\text{SI}} \sim \Omega_{\text{CR}} \frac{n_{\text{CR}}(> E)}{n_i} \left( \frac{v_{\text{st}}}{v_A} - 1 \right) \sim 3 \times 10^{-14} \text{ s}^{-1} \left( \frac{B}{3 \mu\text{G}} \right) \left( \frac{E}{\text{TeV}} \right)^{-1.6}$$

$$(v_{\text{st}}/v_A \sim 2 \text{ and } n_{\text{CR}}(> E)/n_i \sim 10^{-7} (E/\text{GeV})^{1-\alpha}, \text{ with } \alpha \approx 2.6)$$

$$\frac{\gamma_{\text{SI}}}{\nu_{\text{mm}}} \sim 4 \times 10^{-5} \left( \frac{B}{3 \mu\text{G}} \right)^{-1} \left( \frac{E}{\text{TeV}} \right)^{0.4} \left( \frac{l_{\text{mm}}}{100 \text{ npc}} \right)^{-1} \left( \frac{\delta B_{\text{mm}}/B}{1/3} \right)^{-2}$$

➔ With such a large effective collisionality in the system, it is very unlikely that what is, in essence, a collisionless, resonant instability can survive.

2. Let us pretend that the instability is not suppressed:

$$\kappa_{\text{st}} \sim l_c v_{\text{st}} \gtrsim l_c v_A \sim 10^{30} \left( \frac{l_c}{100 \text{ kpc}} \right) \left( \frac{v_A}{100 \text{ km/s}} \right) \text{ cm}^2 \text{ s}^{-1}$$

$$\frac{\kappa_{\text{mm}}}{\kappa_{\text{st}}} \sim 1 \left( \frac{E}{\text{TeV}} \right)^2 \left( \frac{l_{\text{mm}}}{100 \text{ npc}} \right)^{-1} \left( \frac{l_c}{100 \text{ kpc}} \right)^{-1} \left( \frac{B}{3 \mu\text{G}} \right)^{-2} \left( \frac{\delta B_{\text{mm}}/B}{1/3} \right)^{-2} \left( \frac{v_A}{100 \text{ km/s}} \right)^{-1}$$

➔ Scattering of sub-TeV CRs at micromirrors increases the effective CR collisionality in high- $\beta$  environments. This would potentially undermine the CR streaming instability